

CFD investigation of air-water separation using a cavity separator in vertical slug and churn flow

Panopoulos A. Nikolaos

Mechanical Engineering and Aeronautics Dept.
University of Patras
Patras, Greece
panop@upatras.gr

Margaris P. Dionissios

Mechanical Engineering and Aeronautics Dept.
University of Patras
Patras, Greece
margaris@mech.upatras.gr

Abstract—Air-water two phase flow in a vertical rectangular pipe with internal hydraulic diameter of 34 mm is investigated using the CFD code Fluent 16. The VOF multiphase model with the Standard and the RNG k-ε turbulence models are selected. In this study the cavity separator that has been tested only in horizontal flow, is applied on a vertical riser. The results are expressed in terms of air separation efficiency and in air volume fraction iso-surfaces, in different gas and liquid flow rates. Next, the numerical air volume fraction regime results are validated with three regime flow maps and the slug and churn regimes are observed. The conclusions will be used for the construction of the experimental facility for further investigation.

Keywords— air separation; mixture separator; two phase flow; flow pattern map; VOF

I. INTRODUCTION

The simultaneous flow of many phases (gas, solid or liquid) is called multiphase flow. The two phase flow is the simplest case of the multiphase flow. The two distinct phases can be a combination of gas-liquid, liquid-liquid, gas-solid or liquid-solid. The turbulent mixing of the two phases increases the complexity of the mixture flow [1]. The gas-liquid two phase flow is the most common multiphase flow in the oil and gas and chemical industry. Depending on the cross section of the pipe, the mass flow rates, the fluid properties and the orientation of the transportation line it is difficult to predict the distribution of the phases. This is the main reason why the researchers use or design new flow map patterns to describe the mixture flows [2].

In this study a new kind of mixture separator, that is called cavity separator, is applied to the wide side of a vertical pipe with a rectangular cross section of 25x55mm. The principle of operation is simple and is based on the pathetic trapping mechanism that occurs when a cavity is fitted vertical to the flow direction. In previous studies, experimental and numerical investigation has been performed in many different concepts and mixture flow volume supplies for horizontal mixture flow and air separation [3-6]. This numerical study proves at first that the cavity

separator can perform efficiently in low superficial gas velocities.

The next step is the construction of the vertical test section at the Fluid Mechanics Laboratory (University of Patras, Greece) in order to validate the results and to perform series of experiments with one and two separators simultaneous. The classification in the two phase flow field is based on the flow patterns, the void fraction and the pressure drop inside the transportation pipe. The current CFD study is focused on the flow patterns of the air-water vertical flow and the air separation efficiency of the cavity separator “η”. The mixture flow and the separation mechanism result interesting flow patterns which change with the phase superficial velocities. The flow visualization of the air void fraction inside the pipe is presented in terms of air volume fraction isosurfaces using the Fluent 16.0 [7].

II. CFD INVESTIGATION

A. Turbulence Model

The Standard k-ε viscous model was selected for Fluent simulations. The turbulence kinetic energy, k, and its dissipation rate, ε, are obtained from the following transport equations [7].

$$\frac{\partial}{\partial t}(\rho k) + \frac{\partial}{\partial x_i}(\rho k u_i) = \frac{\partial}{\partial x_j} \left(a_k \mu_{eff} \frac{\partial k}{\partial x_j} \right) + G_k + G_b - \rho \epsilon - Y_M \quad (1)$$

This requires a dissipation rate, ε, which is entirely modeled phenomenologically as follows:

$$\frac{\partial}{\partial t}(\rho \epsilon) + \frac{\partial}{\partial x_i}(\rho \epsilon u_i) = \frac{\partial}{\partial x_j} \left[\left(\mu + \frac{\mu_t}{\sigma_\epsilon} \right) \frac{\partial \epsilon}{\partial x_j} \right] + C_{1\epsilon} \frac{\epsilon}{k} (P_k + C_{3\epsilon} P_b) - C_{2\epsilon} \rho \frac{\epsilon^2}{k} + S_\epsilon \quad (2)$$

B. Multiphase Model

The air-water flow regime is simulated with the Volume of Fluid (VOF) multiphase model. The VOF is an Euler-Euler approach for multiphase flow calculation. The VOF model is applied on a fixed Eulerian mesh and is designed for two or more fluids. It was selected because it is able to record in detail the interface between the phases. Some of its applications are the motion of large bubbles in a liquid

or the transient tracking of any liquid-gas interface. It solves a set of n momentum equations for each phase [7]. Geo-Reconstruct scheme is best suited for volume fraction, PISO algorithm is used for the Pressure-Velocity coupling and PRESTO interpolation scheme is used for pressure since gravity is the predominant force acting on the flow. Every other spatial discretization scheme is second order for precision issues while for the accuracy of the solutions, a value of 10^{-4} is used for all residual terms except from the continuity that was set at 10^{-6} . The water-liquid was selected as the primary and the air as the secondary phase. The water density is $\rho_w = 998.2 \text{ kg/m}^3$ and the viscosity $\mu_w = 0.001003 \text{ kg/m}\cdot\text{s}$. The density of the air is $\rho_{air} = 1.225 \text{ kg/m}^3$ and the viscosity is $\mu_{air} = 1.7894\text{e-}05 \text{ kg/m}\cdot\text{s}$.

For each simulation a “Flow rate (kg/s) – Flow time (s)” chart is plotted (Fig. 9). The transient simulation is stopped when the value of the flowrate from the cavity – outlet can be considered as constant value and the mixing flow can be considered as steady state phenomenon.

C. Computational Domain and Grid

The geometry domain under investigation is presented in Fig. 1. It is rectangular duct with rectangular cross section (25x55mm). The hydraulic diameter (D_h) for noncircular pipes is equal to 34 mm. The cavity separator is fitted 340 mm from the mixing tee at the inlet. This distance is equal to 10 times the hydraulic diameter value. The two phases are supplied from different inlet surfaces at the bottom of the pipe. The cavity separator in this study is selected to be a cavity (H: 50 mm, Width: 55 mm and Height: 25 mm) with a circular outlet with value 12.7 mm ($\frac{1}{2}$ inch). The total length of the pipe is 1050mm.

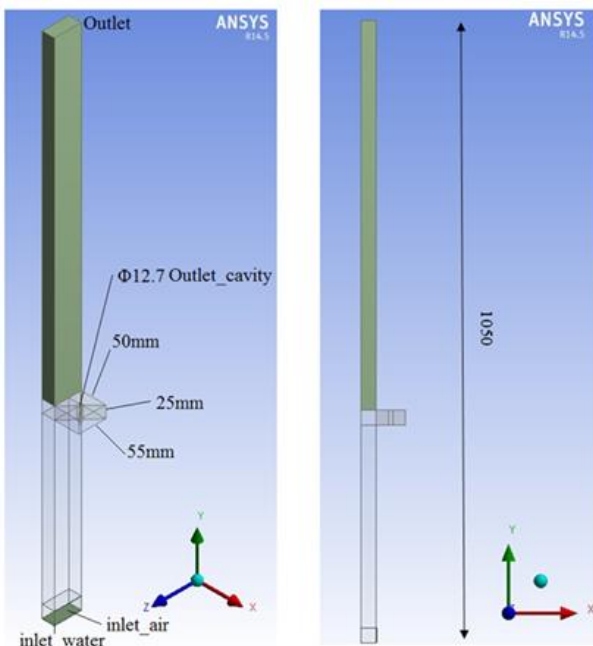


Fig. 1. Computational Domain and dimensions

The geometry was discretized into hexahedral elements. The inflation method was used to generate

a fine grid near the wall. This is done to compute the small fluctuation in fluid property near the wall. The isometric view and the XY plane of the grid is presented in Fig. 2.

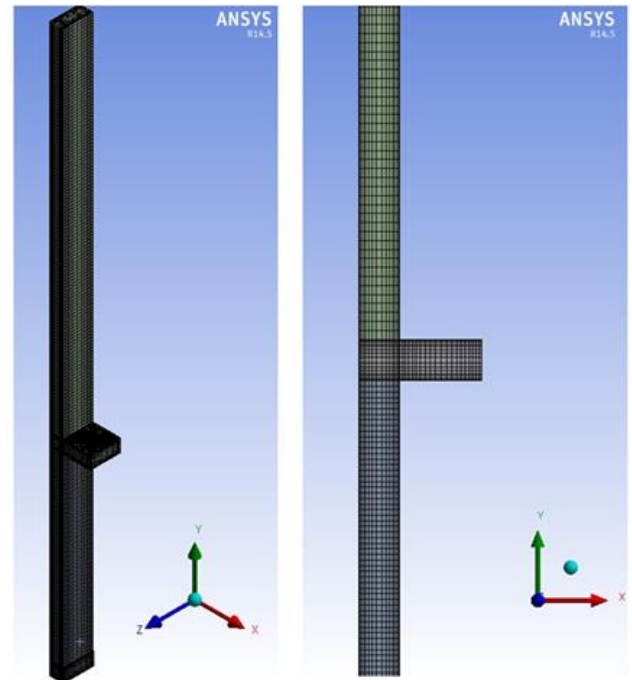


Fig. 2. Numerical Grid (Iso plane – XY plane)

D. Grid independence study

Prior to starting a simulation it must be ensured that the solution is valid and independent of the computational grid. The value of interest in this simulation is the mass flow rate from the cavity outlet. In order to ensure that the numerical grid does not affect the solution four grids were tested under the same boundary conditions. Except from the numerical value, the mass flow rate from the cavity-outlet, the air volume fraction distribution was monitored for each case (Fig. 3). The air volume fraction distribution is the same between the case 3 (108.000 cells) and case 4 (130.000 cells). As a result the grid with the 108.000 cells is selected to proceed to the next simulations.

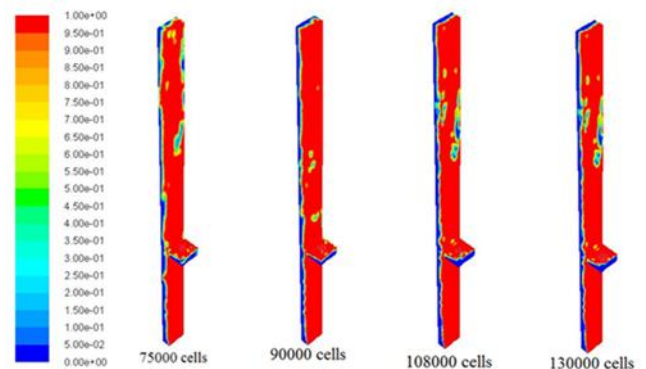


Fig. 3. Air volume fraction distribution testing four grid sizes

III. RESULTS

Three sets of simulations were executed. The water volume flow rates were 1, 1.5 and 2 m³/h with ascending gas flow rate as presented in Tables I, II and III.

TABLE I. BOUNDARY CONDITIONS FOR CASE 1

| Qw: 1 m ³ /h | | | | | |
|-------------------------|-----|---|-----|---|-----|
| U _w (m/s) | 0.2 | | | | |
| U _{air} (m/s) | 0.6 | 1 | 1.3 | 2 | 2.8 |

TABLE II. BOUNDARY CONDITIONS FOR CASE 2

| Qw: 1.5 m ³ /h | | | | | |
|---------------------------|-----|---|-----|---|-----|
| U _w (m/s) | 0.3 | | | | |
| U _{air} (m/s) | 0.6 | 1 | 1.3 | 2 | 2.8 |

TABLE III. : BOUNDARY CONDITIONS FOR CASE 3

| Qw: 2 m ³ /h | | | | | |
|-------------------------|-----|---|-----|---|-----|
| U _w (m/s) | 0.4 | | | | |
| U _{air} (m/s) | 0.6 | 1 | 1.3 | 2 | 2.8 |

In Figures 4 to 8 the air-water mixture flow formation is presented in terms of air volume fraction. These results present the air volume fraction for the case 3, where the water superficial velocity at the inlet is equal to 0.4 m/s (2 m³/h). At the bottom of the pipe there is the mixing tee where the two phases enter the domain. At the bottom where the mixing phenomenon is happening the air tends to occupy the volume towards the front wall surface. In Figure 4 the most important observation is that when the velocities of the two phases are in the same range (0.4 ≈ 0.6 m/s) then the bubble formation occurs at a low level, just above the inlet of the air. Bubbles of different sizes are formatted and travel along the vertical axis. The air volume fraction contour in Fig. 4 proves why the separation efficiency value “η” is higher in the region of low air velocities. More specifically it is observed that a whole air bubble is trapped inside the cavity separator. When the flow pattern consists of big bubbles a periodic separation phenomenon occurs. This is due to the creation of big bubbles one after the other a few centimeters above the air inlet. A fraction of each one enters the cavity and the rest volume rises along the vertical axis towards the main outlet.

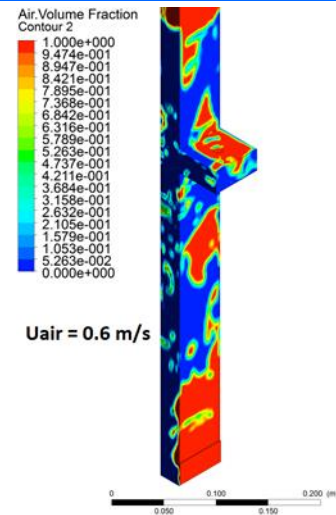


Fig. 4. Air volume fraction – U_{air}: 0.6 m/s - U_w: 0.4 m/s

In Figure 5 the inlet velocity of the air is increased (1 m/s) and the flow phenomena inside the pipe are changed in comparison with the previous case. In fact in this case the formation of the bubbles does not happen just above the inlet but just before the cavity. Moreover, more air volume is trapped inside the cavity. Due to the more air volume at the inlet there is more air quantity in the pipe so bigger air bubbles are observed towards the vertical axis with direction to the vertical outlet.

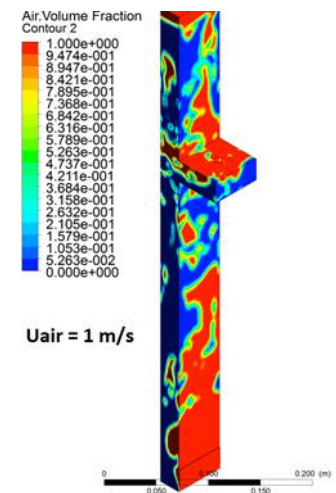


Fig. 5. Air volume fraction – U_{air}: 1 m/s - U_w: 0.4 m/s

The distribution of the air volume fraction when the air velocity is even higher (1.3 m/s) changes again (Fig. 6). In this case it is observed that the cavity is full of air that is trapped inside this deep structure. Moreover the air bubbles are accumulated just before the cavity level. As the air velocity is increased bigger air bubbles are created and lift towards the main outlet at the top of the pipe.

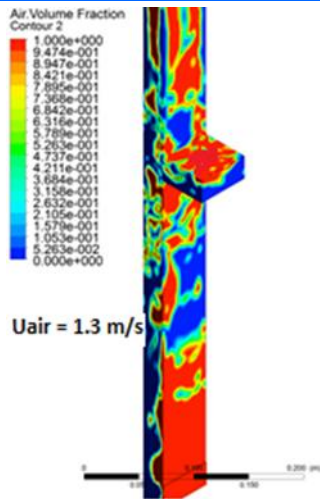


Fig. 6. Air volume fraction – Uair: 1.3 m/s - Uw: 0.4 m/s

Keeping the water volume flow rate constant and increasing the air volume flow rate the volume fraction distribution that is presented in Fig. 7 is created. The main difference in this case is that the air phase does not occupy only the front wall surface but tends to fulfill the short vertical wall surfaces. No big bubbles are observed but a continuous film of air with small water droplets inside.

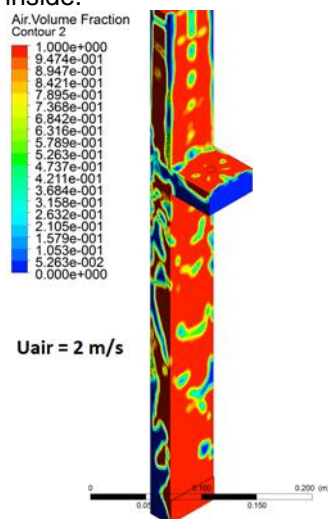


Fig. 7. Air volume fraction – Uair: 2 m/s Uw: 0.4 m/s

The maximum air volume flow rate (2.8 m/s) creates interesting flow phenomena inside the pipe (Fig. 8). Big bullet shaped bubbles are created before the cavity and there is a maldistribution between the two phases. Both phases travel upwards combined in a churn pattern.

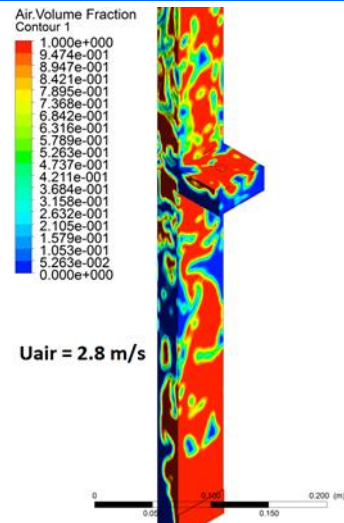


Fig. 8. Air volume fraction – Uair: 2.8 m/s - Uw: 0.4 m/s

IV. RESULTS - COMPARISON

In each simulation a chart similar to the one presented in Fig. 9 was monitored. This mass flow rate fluctuation presents the exported mass flow rate (kg/s) from the cavity outlet as a function of flow time (s). When the exported mass flow rate is almost constant value the simulation is stopped. The numerical values of the chart are integrated and compared to the total air input mass flow to export a mean value of separation efficiency “ η ” (Eq. 3).

$$\eta = \frac{Q_{air,out}}{Q} \quad (3)$$

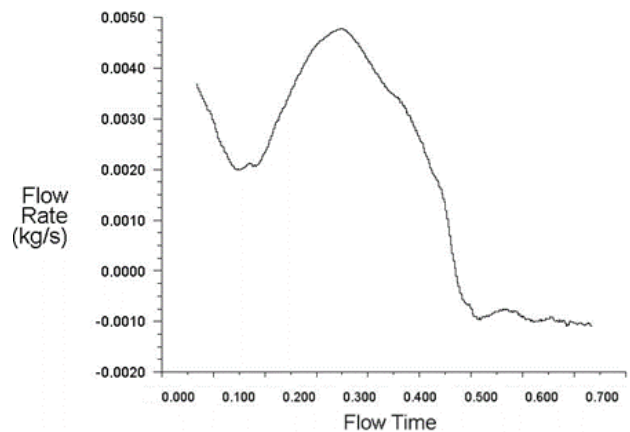


Fig. 9. Mass Flow Rate – Flow Time chart

The Standard and the RNG k- ϵ turbulence models were used for the simulations. Both turbulence models exported similar results as presented in Fig. 10 and 11. More specifically, in each chart the distribution of the air separation efficiency “ η ” is presented as a function of the gas (air) volume flow rate (L/min). In both cases the results lead to the same conclusion. In low water volume rates (1 and 1.5 m³/h) the “ η ” values are in the region of 20%. On the other hand at the 2 m³/h water flow rate the “ η ” values are increased

significantly in the region of 58 – 70%. The higher values occur up to the 1 m/s gas velocity. After that critical value the “ η ” decrease to the region of 20%.

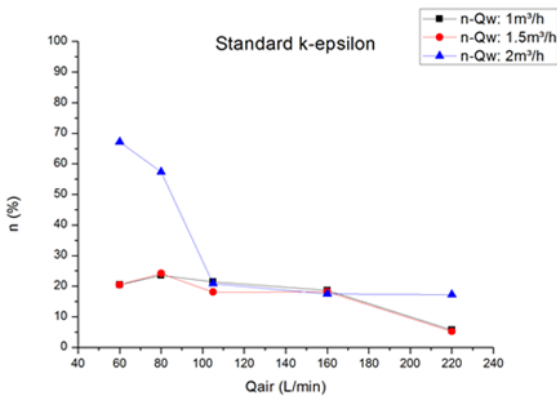


Fig. 10. Air separation efficiency η (%) – Air volume supply (L/min)-Standard k- ϵ

The same conclusion is exported with the RNG k- ϵ turbulence model (Fig. 11).

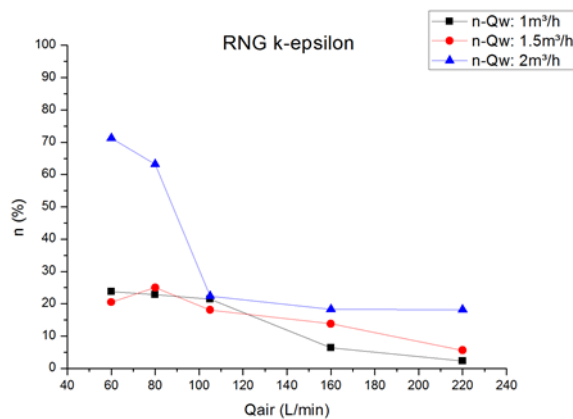


Fig. 11. Air separation efficiency η (%) - Air volume supply (L/min)-RNG k- ϵ

Although the volume fraction results of the Fig. 6 – 8 indicate that when the air velocity is high, the volume of air phase inside the pipe and the cavity is higher, this does not mean that the separation is higher too. The separation is high when the velocities of the two phases are low and almost in the same value range.

V. FLOW PATTERNS

The gas liquid flow is the most common and the most complex multiphase flow because of the combination of the characteristics of the deformable interface with a compressible phase. Different flow rates or different materials result different flow regime which are topological configurations [8]. Figure 12 illustrates the vertical gas/liquid flow patterns. As the ratio of gas to liquid flow rate is increased the transformation is from bubbly flow to disperse flow [9-12].

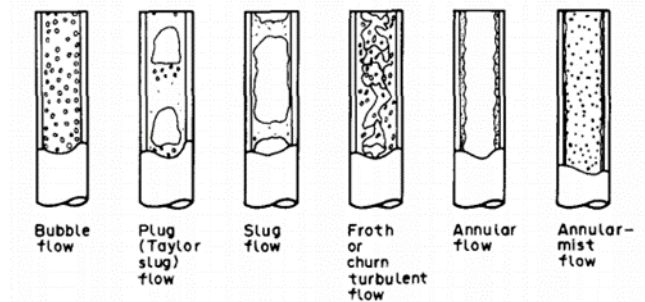


Fig. 12. Flow patterns of gas-liquid flow in vertical tubes [13]

In this study the slug and the churn flow regimes were observed. When the gas flow rate is increased and many bubbles collide and merge to create slugs of gas or larger bubbles the regime is called “slug”. The slug bubbles have characteristic spherical noses and hold almost the whole cross section of the pipe with a thin liquid film separating them from the walls. These gas formulations are commonly named as Taylor bubbles. There are also slugs of water that include small gas bubbles.

As the gas flow rate is increased, the gas velocity causes the destruction of the slug flow pattern and a chaotic type of flow is formatted, the churn flow. In almost every cross section there is a churning motion of gas and liquid volumes [14]. The validation of the air volume fraction distributions is verified by comparing the gas and liquid superficial velocities and the volumetric fluxes with three well known flow maps for gas/liquid vertical flow as presented in Fig. 13 to 15.

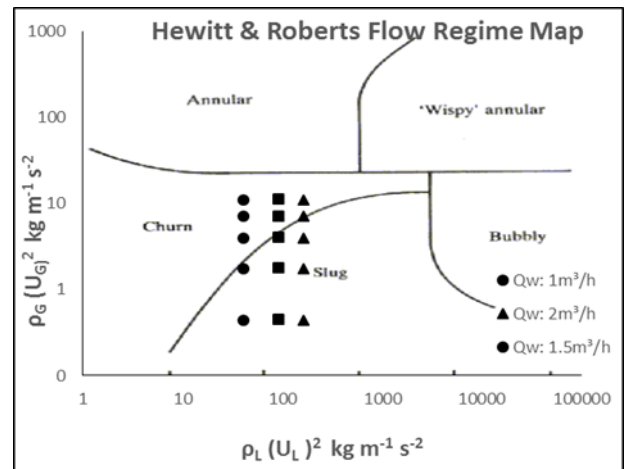


Fig. 13. Hewitt & Roberts Flow Regime Map [15]

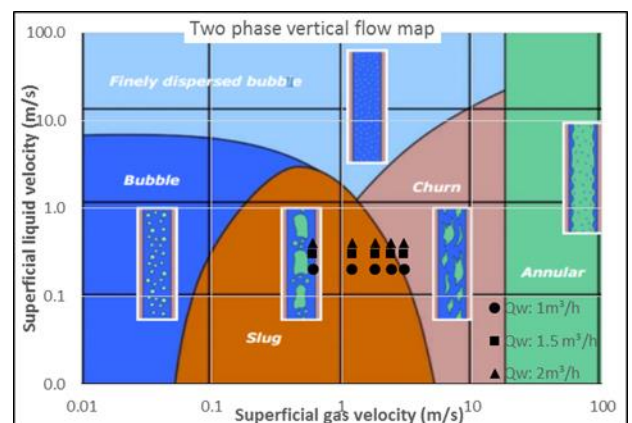


Fig. 14. Two phase vertical flow map [16]

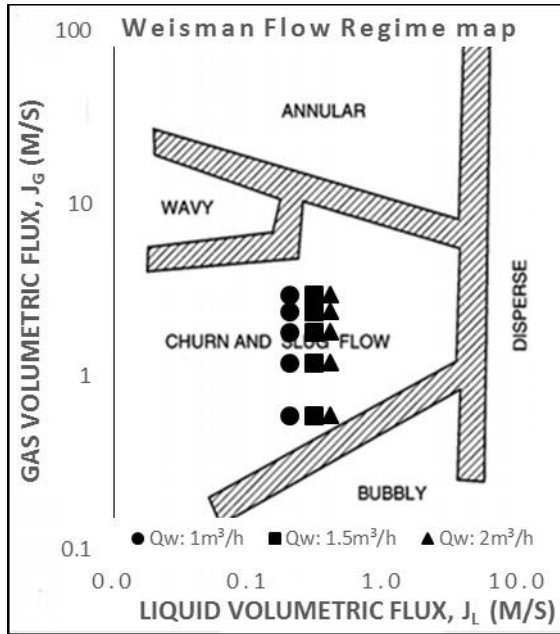


Fig. 15. Weisman Flow Regime Map [17]

VI. CONCLUSION

In this study the application and the efficiency of the cavity separator that was tested only for horizontal flows, is executed using experimental data from previous works [3-6] in a vertical tube with air-water flow. From the above the main conclusions that can be drawn are:

- The flow in the tube with 34 mm hydraulic diameter pipe over range of liquid superficial velocities 0.2, 0.3 and 0.4 m/s and gas superficial velocities of 0.6, 1, 1.3, 2 and 2.8 m/s is the slug and churn flow pattern with the characteristic Taylor bubbles or the chaotic formulations.
- When the liquid flow rate is the maximum for this study (2 m³/h) and the gas superficial velocity is lower than 1m/s the separation efficiency is in the best range of 60-70%.

The next step is the construction of the experimental vertical test section and the investigation of a variety of cases with more than one cavity separators at the same time.

ACKNOWLEDGMENT

The present work was financially supported by the «Andreas Mentzelopoulos Scholarships University of Patras».

REFERENCES

[1] Swanand M.B., "Study of Flow Patterns and Void Fraction In Vertical Downward Two Phase Flow",

Bachelor of Engineering in Mechanical Engineering, Amravati University, May, 2011.

- [2] Sharaf S., Peter van der Meulen, Agunlejika O. E., Azzopardi B., "Structures in gas-liquid churn flow in a large diameter vertical pipe", *International Journal of Multiphase Flow*, Vol. 78, pp. 88 – 103, 2016.
- [3] Panopoulos, N. A., Margaris, D. P., "Experimental And Numerical Analysis Of Air- Water Separation Efficiency Using A Cavity Separator", *Journal of Multidisciplinary Engineering Science and Technology (JMEST)*, ISSN: 2458-9403, Vol. 3 Issue 7, July – 2016
- [4] Panopoulos, N. A., Margaris, D. P., Charalambous A. Y., Pipis P. H., "Experimental Study of Two Phase Flow in a New Proposed Orthogonal Mixture Separator", *International Review of Mechanical Engineering (I.R.E.M.E.)*, Vol. 9, No 6, November 2015.
- [5] Panopoulos, N. A., Margaris, D. P., Kostakontis, G. M., Styliaras, P. E., "Numerical and experimental investigation of air-water two-phase flow in a pipe with three cavities of different aspect ratios", *International Review of Mechanical Engineering (I.R.E.M.E.)*, Vol. 9, No 2, March 2015.
- [6] Panopoulos, N. A., Margaris, D. P., Andriopoulos K. A., "Air separation investigation of gas-liquid stratified - slug flow along horizontal pipe: simulation and experiment", 7th International Conference from "Scientific Computing to Computational Engineering", Athens, July 2016.
- [7] Fluent Inc., *Fluent 15 Documentation-User's Guide*, 2013.
- [8] E. Carpintero Rogero 'Experimental Investigation of Developing Plug and Slug Flows. (Doctoral thesis) Technische Universität, München, 2009.
- [9] Hewitt G.F., Hall-Taylor N.S., "Annular Two-Phase Flow", Pergamon Press Ltd., Headington Hill Hall, Oxford, 1970
- [10] Butterworth D, Hewitt G. F. *Two-Phase Flow and Heat Transfer*. Oxford: Oxford University Press, 1977.
- [11] Hewitt, G. F., "Flow regimes", In *Handbook of Multiphase Flow* (Edited by HETSRONI, G.), Sect. 2.1. Hemisphere/McGraw-Hill, Washington, D. C./New York, 1982.
- [12] Whalley, P. B., "Flooding, slugging and bottle emptying", *Int. J. Multiphase Flow* 13, 723-728, 1987.
- [13] Rouhani S. Z. and M. S. Sohal, "Two-phase flow patterns: a review of research results", *Progress in Nuclear Energy*, Vol. 11, No. 3, pp. 21-259, 1983.
- [14] Wallis, G. B., "One-dimensional two-phase flow", McGraw-Hill Book Company, New York, 1969.
- [15] Hewitt G. F. and Roberts D. N., "Studies of two-phase flow patterns by simultaneous X-ray and flash photography", AERE-M 2159, 1969.
- [16] *Handbook of Multiphase Flow Metering*, Ch. 6, Revision 2, p. 32, March 2015.
- [17] Weisman J. and Kang S. Y., "Flow pattern transitions in vertical and upwardly inclined lines", *Int. J. Multiphase Flow* Vol. 7, pp. 271-291, 1981.